Soft Matter

PAPER

View Article Online
View Journal

Cite this: DOI: 10.1039/c5sm01203a

# Effect of friction on the peeling test at zero-degrees†

Suomi Ponce, José Bico and Benoît Roman*

Received 19th May 2015,
Accepted 17th September 2015

DOI: 10.1039/c5sm01203a

www.rsc.org/softmatter

We describe the peeling of an elastomeric strip adhering to a glass plate through van der Waals interactions in the limit of a zero peeling angle. In contrast to classical studies that predict a saturation of the pulling force, in this lap test configuration the force continuously increases, while a sliding front propagates along the tape. The strip eventually detaches from the substrate when the front reaches its end. Although the evolution of the force is reminiscent of recent studies involving a compliant adhesive coupled with a rigid backing, the progression of a front is in contradiction with such a mechanism. To interpret this behavior, we estimate the local shear stress at the interface by monitoring the deformation of the strip. Our results are consistent with a nearly constant friction stress in the sliding zone in agreement with other experimental observations where adhesion and friction are observed.

## 1 Introduction

Significant efforts have been recently dedicated to the development of adhesives inspired by gecko feet. Indeed, these animals rely on "dry" and reversible adhesion based on van der Waals interactions.[1] However this adhesion is not limited to forces normal to surfaces: geckos not only stand on horizontal ceilings, but may also climb along vertical walls. Friction has been shown to play a major role in the amazing sticking properties of geckos or other animals such as tree frogs.[2–4]

The design of such biomimetic adhesive tapes has motivated the investigation of adhesion in lap-shear configuration (force applied in the direction of the tape) with apparently conflicting approaches. In a recent description, adhesion energy is coupled with the compliance of the system.[5–7] This mechanism leads to the sudden detachment beyond a critical strain. Although this mechanism has been validated experimentally, it challenges the asymptotic limit of a classical model to vanishing peeling angles, where a debonding front progressively propagates as the tape is pulled away.[8–11] However, none of these scenarios involves dissipation through friction. Other studies involving soft adhesive tapes have nevertheless put in evidence a significant effect of friction in a macroscopic region close to the debonding front.[12–17] Other studies finally consider the dissipation induced by the propagation of kinetic waves along the interface.[18]

*Laboratoire de Physique et Mécanique des Milieux Hétérogènes (PMMH), UMR CNRS 7636; Sorbonne Université - UPMC, Univ. Paris 06; Sorbonne Paris Cité - UPD, Univ. Paris 07; PSL - ESPCI, 10 rue Vauquelin, 75005 Paris, France. E-mail: benoit.roman@espci.fr*

† Electronic supplementary information (ESI) available: Movie evidencing the progressive deformation of a strip in shear-lap loading. See DOI: 10.1039/c5sm01203a

In this paper, we wish to study the role of friction in the lap-shear geometry. We are here interested in the pulling of a single strip of silicone rubber adhering to a glass plate through molecular forces. We first clarify in Section 2 the differences and apparent contradictions between the main failure mechanisms described in the literature. We present in Section 3 our experiments conducted with silicone rubber adhering to a glass plate. We put in evidence the propagation of a friction front as the free end of the strip is pulled away. We propose a simple procedure to estimate the characteristic frictional shear stress acting under the elastomeric strip. We finally discuss this friction stress in the light of other studies involving friction with similar materials.

## 2 Lap shear geometry: failure mechanisms

We start by presenting two different scenarios from the literature describing the detachment of a strip adhering to a rigid substrate, when the peeling force is parallel to the substrate (lap shear geometry). In this basic configuration (Fig. 1), a strip of width $w_0$ adheres to the substrate over a length $L_a$, and a force $F$ is applied to the free end of the strip of length $L$ in a direction parallel to the plate.

The first classical approach assumes the propagation of a steady peeling front corresponding to a constant force proportional to the width of the strip and independent of the total adhesion area. Conversely, the second approach assumes an unstable propagation, where detachment takes place in a single dynamical step. In this scenario, the maximum force before detachment depends explicitly on the total adhesive area, Fig. 2. We wish to clarify here the conditions leading to each scenario.

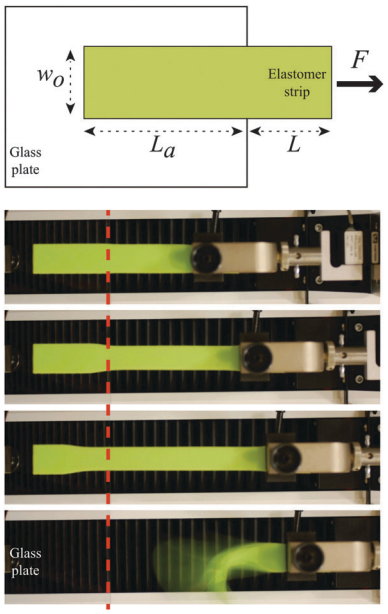


Fig. 1 Top: Sketch of the experimental setup in the initial stage, *i.e.* before any deformation is applied (top view). A long strip of elastomer (in green) of width $w_0$ adheres to a glass plate along a length $L_a$. The pulling force $F$ at the free end of the strip of length $L$ at a constant speed $v$ is monitored with a force displacement machine. Bottom: Snapshots of an actual experiment. The free end is clamped between the moving jaws of the force displacement machine while the glass plate is fixed to the frame. In the last image, the strip has just detached.

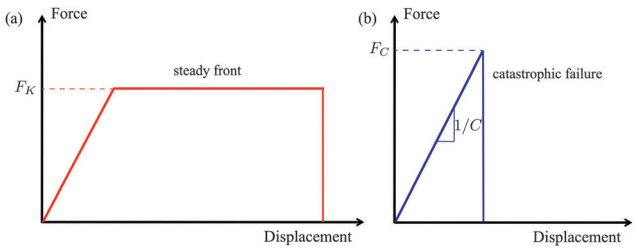


Fig. 2 Complementary scenarios for the failure of an adhesive strip in a lap test configuration. (a) Following the mechanism described by Kendall for a soft strip, a debonding front steadily propagates as the free end of the strip is progressively pulled away (red line). The corresponding plateau force $F_K$ is independent of the length of the strip. (b) In the scenario proposed by Crosby *et al.*, elastic energy is first stored in the system of compliance $C$ and suddenly released as it reaches the critical debonding energy (blue line). The critical load $F_C$ is in this case dependent on the length of the adhering strip.

### 2.1 Steady detachment front

In a classical derivation, Kendall[10] considered the steady peeling of an elastic strip of width $w_0$, thickness $h$ and Young's modulus $E$, adhering to a rigid substrate with an adhesion energy $\gamma$ (note that $\gamma$ does not correspond to the thermodynamic adhesion but may depend on the dynamics and the details of the loading at the debonding front). Friction is not considered in this calculation, *i.e.* $\gamma$ is assumed to be independent of the detachment mode (in terms of classical fracture terminology, we neglect mode mixity[19]). In a steady regime, the operator applies a constant pulling force $F = Ehw_0\varepsilon$, which stretches the strip to a strain $\varepsilon$. The elastic energy stored in the strip is then $F^2/2Ehw_0$ per unit length. In the limit of the vanishing peeling angle, the operator displaces the free end of the strip by a quantity $\varepsilon dx$ as the delamination front advances by a distance $dx$ and thus provides a work $\delta W = F\varepsilon dx$. This work is transformed into adhesion energy $\gamma w_0 dx$ but also increases the strechting energy stored in the elastic strip $(F^2/2Ehw_0)dx$. Energy conservation leads to the steady pulling force:

$$F_K = \sqrt{2Eh\gamma}w_0 \quad (1)$$

This expression is in agreement with the experiments presented in Kendall's study for angles as low as 10° conducted with ethylene propylene rubber strips adhering to glass through molecular forces.[10] Since the stretching of the strip is important for low peeling angles, standards for testing tapes usually involve large angles of 90° or 180° for which the peeling force is simply proportional to the adhesion energy. As a consequence, studies testing the same lap shear regime with different systems are rather scarce in the traditional literature on adhesion.

### 2.2 A scenario for catastrophic debonding

Motivated by the design of biomimetic adhesives, Crosby and coworkers developed a different concept based on catastrophic detachment to predict the adhesive force capacity in a general configuration.[5,6] The main argument is that the system of compliance $C$ stores an elastic energy on the order of $CF^2$ as it is loaded with a force $F$. This energy is compared with the cost $\gamma_s A$ for debonding an area $A$. Note that $\gamma_s$ corresponds to the critical energy release rate under shear (fracture mode mode II). As the force is progressively increased, the elastic energy eventually reaches the energy required for a total debonding. The situation becomes unstable even if the load is applied through an imposed displacement and the adhesive suddenly detaches beyond the critical load:

$$F_C \sim \sqrt{\gamma_s A/C}. \quad (2)$$

Although neither the friction nor the kinetic energy generated by the propagation of the fracture are considered in this approach, this relation is nicely verified in a wide range of experiments involving a compliant elastomer coated with a stiff fabric backing. Interestingly, the failure load obtained in such experiments yields a shear debonding energy $\gamma_s$ about one order of magnitude greater than the adhesion energy $\gamma$ obtained in a peeling test at 90 degrees.[20]

The scaling relation (2) is a general result regarding the case of catastrophic debonding. Examples of its application to different geometries involving a backing and a soft adhesive are reviewed by Bartlett *et al.*[6] We present here as an illustration the case of an adhesive elastomer (of thickness $h$ and width $w_0$) covered with an inextensible backing in the same geometry as in Fig. 1. If a load $F$ parallel to the strip is applied, the backing is translated as a rigid body along a distance $\delta$, which induces a uniform shear strain $\delta/h$ in the portion of the elastomer adhering to the rigid substrate. The elastic energy stored in the

system is therefore $\mu h(\delta/h)^2/2$ per unit of bonded area, where $\mu$ is the shear modulus (in the case of an incompressible elastomer, $\mu$ is simply one third of the Young's modulus, $\mu = E/3$). In a steady state propagation, an advance of a debonding front over a distance d$x$ will release $\mu h(\delta/h)^2 w_0 \mathrm{d}x/2$ of elastic energy, with a cost $\gamma w_0 \mathrm{d}x$ of fracture energy. As a consequence, the front will propagate in a single step along the whole extent of the sample if the imposed displacement $\delta$ is larger than $\delta_c = \sqrt{2\gamma h/\mu}$. This threshold corresponds to a shear stress on the adhesive $\mu\delta_c/h$ and results in a critical load $F_C = \mu L_a w_0 \delta_c/h$. Eqn (2) is finally recovered:

$$F_C = \sqrt{2\gamma_s A/C} = A\sqrt{2\mu\gamma_s/h} \qquad (3)$$

where $A = wL_a$ is the adhesion area and $C = h/\mu w L_a$ is the compliance of the system.

However if we directly apply eqn (2) to the first system (strip without backing), we do not recover eqn (1). Indeed, the compliance of the system before detachment is given by $C = L/(Ehw)$, where $L$ is the length of the free portion of the strip since the adhering part of the strip first remains undeformed. Eqn (2) would thus lead to a different result‡ $F_C = \sqrt{2Eh\gamma_s} w_0 \sqrt{L_a/L}$. This is not surprising, since the basic assumptions on the failure mode are different (steady progressive detachment *versus* a catastrophic single event).

### 2.3 Reconciling contradictory mechanisms

Which mode of failure occurs in the case of a strip of soft elastomer covered with a rigid backing? Considering the finite stiffness of the backing can reconcile both approaches.

The strain in the strip is uniform in the detached side, and vanishes in the adhered part after a progressive transition of extension $\ell_{lag}$ (see Fig. 3). We now estimate $\ell_{lag}$ as a function of the mechanical properties of the backing tape and the elastic strip (in the absence of backing $\ell_{lag}$ should be on the order of the thickness of the strip $h$). We assume that the backing is much stiffer than the elastomer, *i.e.* $Eh \ll E_b h_b$, where $E_b$ and $h_b$ are the Young's modulus and the thickness of the backing material. Within this limit, the elastic strip is mainly subjected to a simple shear, whereas the stiff backing undergoes stretching. A simple force balance on a short portion of the strip leads to

$$\frac{E}{3h}u + E_b h_b \frac{\partial^2 u}{\partial x^2} = 0,$$

where $u(x)$ is the local displacement of the tape at position $x$. As described by Kaelble,[9] the integration of this equation leads to an exponential decay of the strain of the strip over a distance:

$$\ell_{lag} \sim h\sqrt{\frac{E_b h_b}{Eh}}. \qquad (4)$$

Comparing $L_a$ with $\ell_{lag}$ indicates which debonding mechanism we should expect. If $\ell_{lag} \gg L_a$, the whole adhesive layer is under uniform shear. We recover a situation similar to the case of inextensible backing and the strip should suddenly detach beyond the critical load $F_C$.

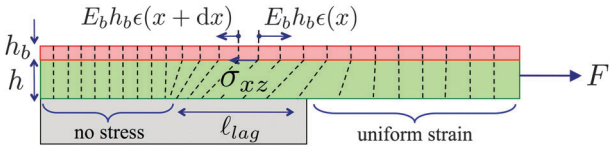


Fig. 3 A case of a strip coated with a backing of finite rigidity. The coupling between the tensile strain in the backing and the shear in the soft adhering strip results in the decay of the local strain along a length scale $\ell_{lag}$.

Conversely, in the case of $\ell_{lag} \ll L_a$, a small fraction of the strip adhering to the substrate is subject to the applied load. The remaining part of the strip remains at rest in agreement with Kendall's steady scenario, leading to a steady load $F_K$ (eqn (1)). This would, for instance, be the case in the absence of a backing layer, where $\ell_{lag} \sim h$.

As a conclusion, the mode of failure is selected by the length of the adhered zone $L_a$ compared to the shear elastic decay length $\ell_{lag}$. Longer adhered areas will eventually reach Kendall's plateau (eqn (1)), whereas shorter ones (or very stiff backing) will follow a catastrophic scenario (eqn (2)).

However, although friction obviously prevents the tape from sliding, none of these mechanisms accounts for a possible energy dissipation through friction. The effects of friction in peeling configurations have nevertheless been evidenced and described at both local[12–14] and global scales.[15–17]

In the following section, we present experiments with a strip made with a single material where friction plays a major role. Curiously, we observe a propagating front reminiscent of Kendall's mechanism but the force leading to the detachment of the strip is proportional to the initial adhesion area, as in the catastrophic scenario.

## 3 Experiments with silicone rubber adhering to glass

### 3.1 Experimental methods

Our experiments were performed on smooth glass plates carefully cleaned with ethanol. The strips made of polyvinylsiloxane (Elite Double 16, 22 and 32 from Zhermack) were prepared by mixing equal quantities of "base" and "catalyst" liquids. The strips were elaborated with an initial length of 250 mm, a width $w_0$ ranging from 7.5 to 60 mm, and a thickness $h$ of 1 or 2 mm. The Young's modulus could be selected between 400 and 1200 kPa. Accidental dust particles were removed using a standard adhesive tape. The strips spontaneously adhere to glass through intermolecular interactions.

The adhesion energy was measured for each sample through a standard 90° peeling test[21] carried at a velocity of 0.5 mm s$^{-1}$ using an Instron 5865 force–displacement machine. Depending on the polymer selected, $\gamma$ could vary between 0.5 and 1.5 N m$^{-1}$. Following the procedure described by Crosby *et al.*, we finally

‡ We note however that in many cases $L$ and $L_a$ are of the same order of magnitude so that the scaling relation (2) applies again.

performed some experiments with strips covered with a stiff backing, in which case the debonding is catastrophic. We obtained a shear debonding energy $\gamma_s$ ranging from 1.4 to 5.4 N m$^{-1}$ (the experimental procedure is described in Section 3.6.2).

Before starting a lap-test experiment, a strip of length $L_a$ is deposited on the glass plate. After a waiting time on the order of 5 min, the extremity of the free portion of the strip was clamped between the jaws of the force displacement machine and was pulled at a constant velocity $v$ ranging from 10 to 50 mm min$^{-1}$, while the glass plate is held at a fixed position (see Fig. 1). The alignment with the glass plate was verified with a laser sheet projected on the strip with a low incidence. A finite peeling angle would result in a deflection of the projected line. This setup ensured that the peeling angle was less than 0.7°. Moreover, supplementary experiments conducted at low but finite peeling angles did not significantly change the results. The pulling force $F(t)$ and the displacement of the free end $\delta(t)$ are simultaneously monitored. For a given set of experiments, the compliance of the non-adhering portion of the strip was maintained constant. This means that the initial length had a fixed value of $L = 40$ mm in most of our experiments, so in order to vary $L_a$, we vary the total length of the strip.

### 3.2 Peeling force

Following the previous studies described in Section 2, we would expect to obtain a constant plateau for the peeling force since the strip is not covered with any backing ($L_a \gg \ell_{lag} \sim h$). However, our experimental results are in contradiction with this scenario. We indeed observe a continuous increase of the force as the free end is pulled away until the strip detaches (Fig. 4). In addition, the critical force for detachment increases with the adhered area (here with length $L_a$), and its value (up to 40 N) is much higher than the critical force predicted by Kendall $F_K = 1.5$ N for $\gamma \approx 1$ J m$^{-2}$ in eqn (1). Finally note that prior to detachment, the force sometimes displays jumps as it is commonly observed in systems displaying stick-slip behaviors.

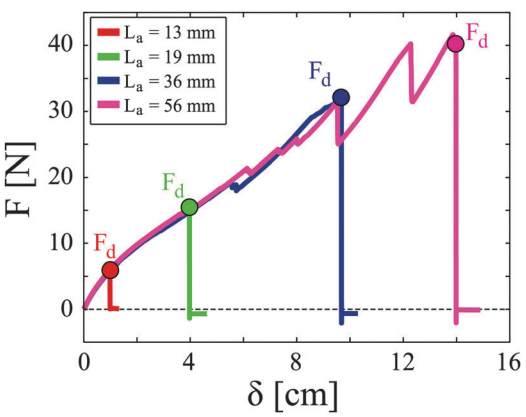


Fig. 4 Tensile force applied to the strip as a function of the imposed displacement. The material parameters of the strip are $E = 529(\pm 2)$ kPa, $L = 49$ mm, $w_0 = 30$ mm, and $h = 2.3$ mm. The detachment force is marked for each experience with a point of the same color of the corresponding adhering length.

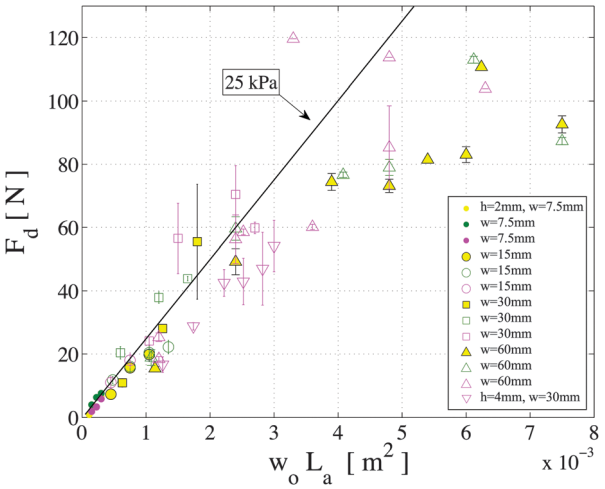


Fig. 5 Force at the detachment of the strip as a function of the initially adhering area, ● for $w_0 = 7.5$ mm, ○ for $w_0 = 15$ mm, □ for $w_0 = 30$ mm, △ for $w_0 = 60$ mm. The color code corresponds to the Young's modulus: $E_{magenta} = 520(\pm 50)$ kPa, $E_{yellow} = 730(\pm 160)$ kPa and $E_{green} = 1130(\pm 160)$ kPa (the variability in $E$ is related to different specimens).

At first glance, the evolution of the force is reminiscent of the mechanism described by Crosby and coworkers.[5] However, an estimate of the corresponding force as predicted from eqn (2) leads to $F_C \approx 2$ N, for an area $A = w_0 L_a = 10^{-3}$ m$^2$, a debonding energy of $\gamma_s \approx 5$ J m$^{-2}$ and compliance $1/C \approx 300$ N m$^{-1}$ directly inferred from Fig. 4. This estimate is more than one order of magnitude lower than the detachment force actually measured ($F_d \sim 40$ N), which would require an unrealistic value of $\gamma_s \sim 2$ kJ m$^{-2}$.

To gain further insight, we performed similar experiments with strips of different geometries and elastic rigidities. We represent in Fig. 5 the maximum load obtained for these experiments as a function of the initially adhering area. Both quantities are fairly proportional, independent of the width and the thickness of the strip or even the Young's modulus of the elastomer. Our data suggest that the detachment force obeys

$$F_d = \tau_{eff} w_0 L_a = \tau_{eff} A, \quad (5)$$

where the prefactor $\tau_{eff}$ has the dimension of a stress and is on the order of 20–30 kPa in our system.

Nevertheless, monitoring the total force only provides a very limited analysis. In the following section we describe the local strain distribution in the strip through a simple imaging technique, and describe the propagation of a sliding front.

### 3.3 Local friction

**3.3.1 Front propagation.** We present in Fig. 6 successive snapshots of a strip captured during an experiment (see also the movie in the ESI†). When the strip is stretched, its width decreases as a consequence of the incompressibility of the elastomer (the Poisson coefficient is close to 0.5 for such materials).

Three different zones are clearly identified by following the local width $w$ of the strip, see Fig. 6 bottom. In zone 1, the strip

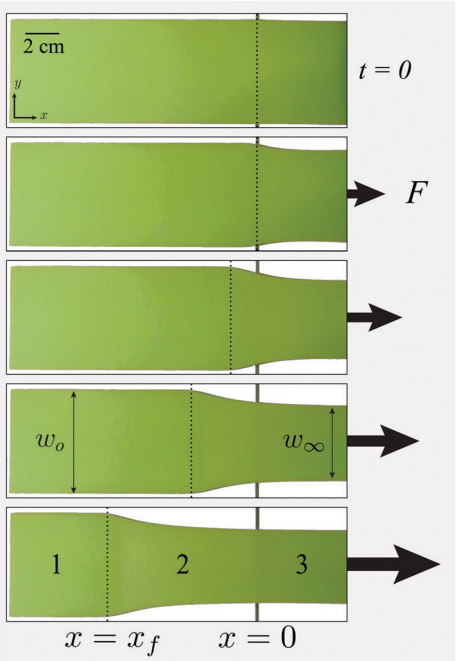


Fig. 6 Experimental snapshots of the strip during successive instants of an experiment (a movie of the experiment is available as ESI†). Transition region 2 can be clearly identified between region 1, where the strip is at rest, and region 3, where the strip is away from the glass plate and uniformly stretched. The deformation front which is separating regions 1 and 2 advances towards region 1 as the strip is continuously pulled away. Here, $w_0$ = 60 mm.

adheres to the glass plate and does not experience any stress. Zone 3 is the part of the strip that is away from the plate. The width $w_\infty$ is uniform in this zone, indicating a constant extension stress along the strip ($w_\infty < w_0$). Zone 2 corresponds to a transition between zones 1 and 3. The width $w(x)$ varies gradually along this region from $w_0$ to $w_\infty$. This evolution indicates that the tension in the strip progressively decays from zone 3 to zone 1.

A sliding front delimits zones 1 and 2. This front of position $x_F$ propagates towards zone 1 as the end of the strip is continuously pulled away. The strip eventually detaches when this front gets close to its end, and the whole strip coils back.

**3.3.2 Friction stress along the strip.** As the deformation front propagates, we observe that in zone 2 the strip remains in contact with the glass plate, sliding over it, which indicates that the adhering material is subject to friction. We propose in this section to estimate directly the shear stress acting on the strip by measuring its lateral deformation.

Due to the symmetry of the deformation profile and the horizontal direction of the pulling force, the global force $F(x)$ acting on a transverse slice of the material is also horizontal and directed along the $x$ axis. Zone 1 of the strip is free from any stress, while zone 3 is under uniform axial stress, $\sigma_{xx} = F_\infty/w_0h$. In zone 2, $F(x)$ varies from 0 to $F_\infty$ and we assume that the strip is subjected to a shear stress as a result of frictional sliding. We refer to $\tau(x)$ as the value of this shear stress averaged over the local width $w(x)$. If we neglect the stresses and strains in the

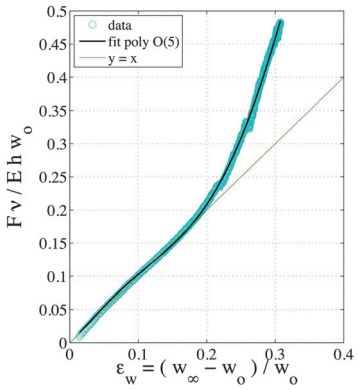


Fig. 7 Calibration curve of the force as a function of the width of the strip. The initial linear dependence provides the Young's modulus of the material (in the current case, 1 MPa). The black solid curve corresponds to a 5th order polynomial fit and the green solid line is the reference of a linear curve with unit slope.

$y$ direction, a simple force balance connects $\tau$ to the evolution of the global force $F(x)$ acting on a slice of the strip:

$$\frac{\partial F}{\partial x} = w(x)\tau(x). \qquad (6)$$

In order to estimate the local force $F(x)$, we extract the corresponding local width $w(x)$ from image processing, and compare it with a calibration curve determined through a standard force *vs.* displacement test implemented with a synchronized imaging of the strip. In this approach, we assume the relationship between $F(x)$ and $w(x)$ to be locally the same as in a uniform tensile test although the strain varies spatially. Neglecting the two dimensional effects is in principle valid for slowly varying loads, an assumption which can be questioned in our experiments, especially in the vicinity of the sliding front. The elastomer follows a Hookean behavior for moderate strains up to $\varepsilon_w = (w - w_0)/w_0 \sim 0.2$ and hardens for higher strains (Fig. 7). We used a 5th order polynomial fit to account for this non-linear behavior. By simply following the evolution of $w(x)$ we thus infer the local tension $F(x)$, and using eqn (6) the shear stress $\tau(x)$ acting on the strip is computed.

Fig. 8 represents, at a given time, the spatial dependence of the width of the strip, the local force deduced from the calibration and the frictional shear stress estimated from eqn (6). As is expected, $\tau(x)$ starts from zero in zone 3, increases in zone 2 and eventually vanishes again in zone 1.§

Interestingly, the shear stress reaches a constant value on the order of 40 kPa. The same procedure can be repeated at successive moments of the experiment. The global evolution of the stress distribution $\tau(x)$ is best visualised using a space–stress diagram (Fig. 9). The imposed displacement is measured directly by the traction machine and is proportional to time, since the displacement speed is imposed to 0.5 mm s$^{-1}$ in the presented experiments. This particular experiment has been

§ Note that our technique leads to a non-zero value of $\tau(x)$ in zone 3 in the vicinity of the edge of the glass plate. We interpret this artefact as a consequence of strains in the $y$ direction that we have neglected.

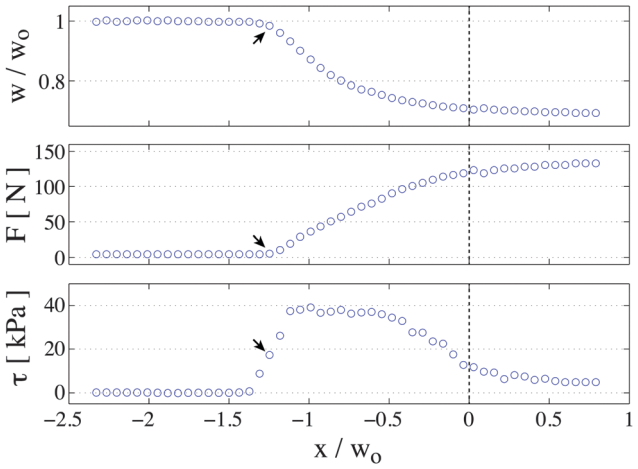


Fig. 8 Measurement of the local width and estimation of the corresponding force and shear stress acting on the strip at a given time (the applied displacement corresponds to $d/w_0$ = 2.33 in Fig. 9). In the $x$ coordinate, zero corresponds to the edge of the glass plate, while positive coordinates represent the side of the strip that is peeled away from the plate, *i.e.* zone 3. The arrows indicate the position of the sliding front $x_F$. This front is defined as the location where the local width has decreased by 1% from its initial value. Experimental parameters are: $E$ = 1055 kPa, $h$ = 2.2 mm and $w_0$ = 60 mm.

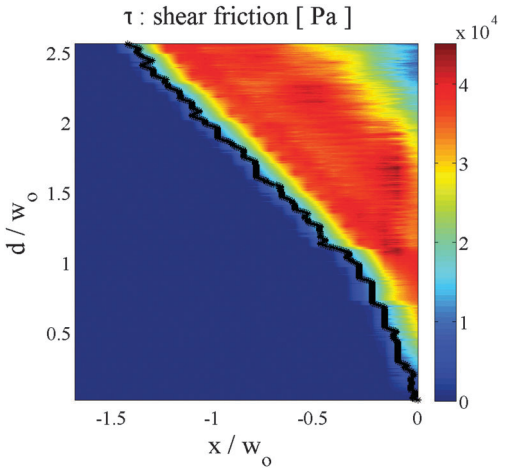


Fig. 9 Space–displacement diagram representing the estimated shear stress acting on the strip as its free end is pulled at a constant velocity. Experimental parameters: $E$ = 1055 kPa, $h$ = 2.2 mm and $w_0$ = 60 mm. The sliding front represented by the black line progressively propagates through the strip. Data in Fig. 8 correspond to $d/w_0 \sim 2.33$ in the space–displacement diagram.

conducted with $E$ = 1055 Pa, $L_a$ = 140 mm, $w_0$ = 60 mm, and $h$ = 2.2 mm. Nevertheless, similar qualitative features were obtained with other specimens. In particular, we found a plateau shear stress in the range 20 to 40 kPa for all the strips.

Recent studies have been specifically dedicated to the friction between soft polydimethyl siloxane (PDMS) and rigid materials (glass with different molecular coatings). In these experiments, a spherical cap made of PDMS is slid over a glass plate.[22,23] Conversely, a glass spherical cap can also be put in contact with a flat substrate of PDMS with a fixed normal load and subjected to a given torsional stress.[24–28] Peeling configurations closer to the present study have also been explored through the tracking of markers embedded in the tape.[13,14] As a salient result, sliding involves a constant frictional shear stress independent of pressure in the case of smooth contact, in contrast to the common Ammonton–Coulomb law. Friction stresses were found to depend significantly on the chemical treatment of the interface and, to a lower extent, on the sliding velocity. Nevertheless their values all range between 10 and 500 kPa. Although the chemical nature of the polyvinylsiloxane rubber used in our experiments is slightly different from PDMS, our data are compatible with previous studies.

In order to test the possible influence of the chemical nature of the substrate, we conducted two additional series of experiments with glass plates grafted with trichloroperfluorooctylsilane and with adsorbed polydimethylsiloxane molecules (PDMS, viscosity of 200 cSt). Both treatments are indeed commonly used to modify surface energies and are described in detail by Mettu and Chaudhury.[29] Lap-test experiments exhibited the same qualitative behavior as in the case of a clean glass plate. The different values for the adhesion energy $\gamma$, the shear debonding energy $\gamma_s$ and the friction stress $\tau$ obtained with the same polymer ($E$ = 1300 kPa) and the same pulling velocity (0.5 m s$^{-1}$) are reported in Table 1. As a general trend, both treatments significantly decrease adhesion energies and more moderately the friction stress. Stronger effects are obtained for the plate coated with PDMS. A deeper interpretation of this comparison is however beyond the scope of the present work.

### 3.4 From local friction to the global peeling force

The integration of the local friction stress described in the previous paragraph provides the global pulling force, $F = \int_0^{x_F} \tau(x) w(x) \mathrm{d}x$. In the previous section, the friction stress was found to quickly reach a plateau value as the sliding front progresses. Multiplying this plateau value by the contact area should thus provide a good estimate of the force. As a first order approximation, the contact area is equal to $x_F w_0$ with an error below 20%, leading to a pulling force proportional to the displacement of the sliding front. This linear variation is approximately observed in our experiments and corresponds to an average friction stress of 30 kPa (Fig. 10a). The detachment force follows the same evolution, which indicates that the band detaches when the front reaches its extremity (Fig. 10b). In practice, the strip actually detaches before the front reaches the free end of the strip, probably because this front is not perfectly straight.

However, the details of the evolution of the pulling force with the position are in reality more subtle than a linear relation

Table 1 Adhesion energies and friction stresses obtained with the same polymer ($E$ = 1300 kPa) on different substrates. A clean glass is compared with a glass grafted with trichloroperfluorooctylsilane and with adsorbed polydimethylsiloxane molecules (PDMS, viscosity of 200 cSt)

| Surface | $\gamma$ [N m$^{-1}$] | $\gamma_s$ [N m$^{-1}$] | $\tau$ [kPa] |
|---|---|---|---|
| Plain glass | 0.8 ± 0.1 | 5.3 ± 0.5 | 65 ± 5 |
| Perfluorosilane | 0.54 ± 0.08 | 4.7 ± 0.5 | 48 ± 2 |
| PDMS | 0.36 ± 0.04 | 2.6 ± 0.5 | 39 ± 4 |

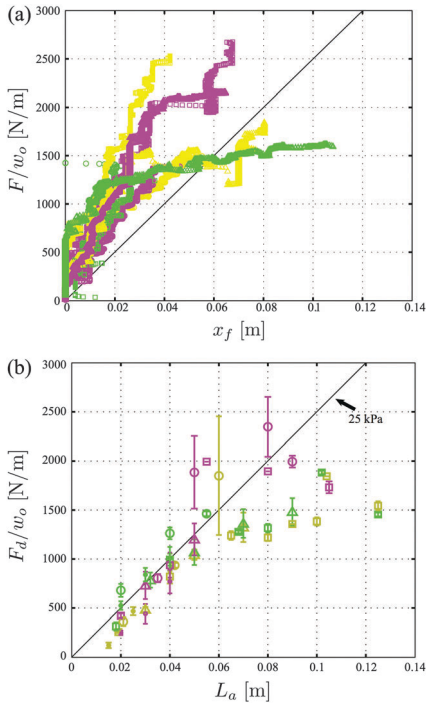


Fig. 10 (a) Instantaneous applied force normalized by the initial strip width as a function of the detachment front position. (b) Final detachment force normalized by the strip width as a function of the initially adhered length. The legend for both figures is the same as in Fig. 5, except curves for $w_0$ = 7.5 mm are not presented. The solid black line represents a stress of 25 kPa.

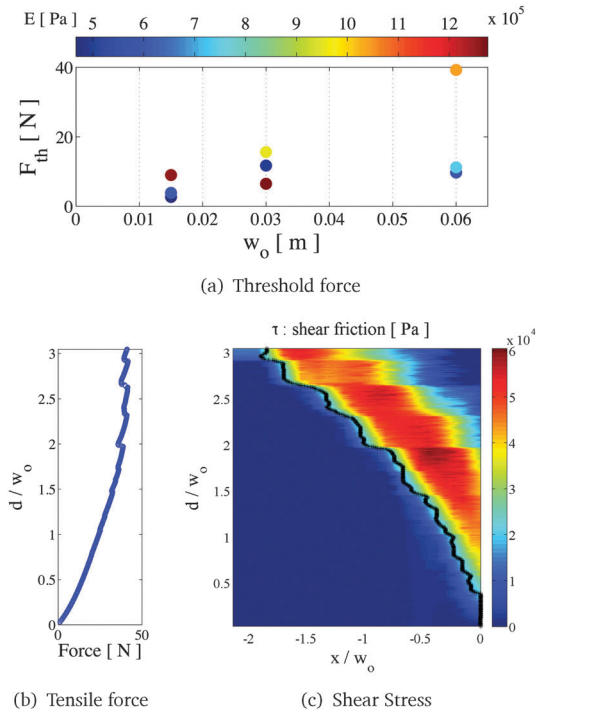


Fig. 11 (a) Threshold force as a function of the width of the strip. The colorbar represents the Young's modulus of each sample in units of Pa. (b) Evolution of the tensile force as a function of the imposed displacement in an experiment displaying stick-slip behavior (upwards). (c) Space–stress diagram quantifying the corresponding shear stress on a strip, the black line represents the sliding front position. Sample parameters for diagrams (b) and (c): $E$ = 1055 kPa, $h$ = 2.2 mm and $w_0$ = 30 mm.

relying on a fixed value of the friction stress. We indeed observe a threshold of force below which the front does not move. Stick-slip motion of the front is also observed for high strains. In this case the force tends to saturate, especialy for wide strips. We describe both effects in the following section.

### 3.5 Before and beyond steady sliding

**3.5.1 Sliding threshold.** In our experiments, the sliding front is only observed to move beyond a critical pulling force $F_{th}$, as shown in Fig. 10a. The critical force is approximately proportional to $w_0$, which corresponds to a critical tension $F_{th}/w_0$ on the order of 330 N m$^{-1}$ (Fig. 11a). This threshold is not included in our description involving a sliding front. In this model, the strip is indeed expected to start sliding for any finite pulling load.

This critical tension could be intuitively compared with the law predicted by Kendall (eqn (1)), where the peeling front is also expect to move beyond a critical load. However, the numerical estimates of $\sqrt{2Eh\gamma}$ lay within the range 30 to 50 N m$^{-1}$ for our configuration, which is low in comparison with the tension $F_{th}/w_0$ we measured in our experiments. The use of shear debonding energy $\gamma_s$ may be more relevant than the adhesion energy $\gamma$. Nevertheless, it would increase the estimate to a maximum value of 100 N m$^{-1}$, which remains too low compared to the expected 330 N m$^{-1}$.

Another candidate for the threshold would be the product $\tau\ell$ of the friction stress with a length scale $\ell$. In our simplified approach, the details of the shear across the thickness of the strip were indeed not considered. However, we expect the strain distribution to evolve from a uniform axial strain to a uniform shear in the vicinity of the edge of the plate. Due to the Laplacian nature of elasticity equations, the length scale involved is set by the thickness of the strip $h$. Nevertheless, the product $\tau h$ is on the order of 50 N m$^{-1}$. This value also appears too low, even if a numerical prefactor might increase the actual effective length scale.

Two-dimensional effects were finally neglected in our simplified approach. However, the sides of the strip tend to slide toward the center line as the strip is stretched. In more pronounced situations this lateral displacement leads to the evolution of the peeling front into a V shape.[18] The coupling of the shear in both directions may also explain the premature detachment of the strip before the friction front reaches $L_a$. The consequence of such 2D effects would lead to a length scale $\ell$ proportional to $w_0$. Numerically the product $\tau w_0$ varies in the range 300 to 1800 N m$^{-1}$ in our experiments, which now tends to be too high. Besides we would then expect a quadratic variation of the critical force with the width, which contradicts our observation (although the actual data are scattered).

To conclude, although the details of the critical force remain an open question, its value should rely on a combination between the details of shear strain and 2D effects.

**3.5.2 Stick-slip.** We present in Fig. 11b and c, a force-displacement curve and the corresponding space–stress diagram

where jumps are clearly evidenced. Interestingly, the whole sliding zone is globally shifted for major jumps. This shift leads to the development of a secondary front in the rear part of the strip remaining in apparent contact with the rigid plate. The shear stress significantly decreases and almost vanishes in this region. As a consequence, the force tends to saturate as observed in Fig. 10 for high pulling forces. The observed stick-slip behavior, also noticed by Lake and Stevenson[18] in a peeling configuration, is reminiscent of Schallamach waves.[30,31] Qualitatively, stick-slip appears for high strains and is very sensitive to minute air bubbles trapped between the strip and the plate. A quantitative description of the phenomenon is beyond the scope of the current study. Understanding stick-slip behavior is nevertheless crucial for practical applications since it may lead to a premature detachment of the bond.

### 3.6 Comparison with other experiments

**3.6.1 Towards adhesion rheology?** Although the experimental procedure is very close to the study by Kendall,[10] the results are significantly different. Both situations indeed involve the propagation of a front, but the case of Kendall does not include friction, which leads to a steady peeling force even in the limit of a vanishing peeling angle. Conversely, the propagation of a sliding front results in an increasing force in our experiments. If the specimens are long enough, the detachment force is several orders of magnitude higher than the prediction by Kendall. Recent experiments conducted with strips of polydimethylsiloxane adhering to glass also involve important frictional dissipation at low peeling angles.[15] Similar large effects of friction for low angles are also observed in our system.[32] However, the reason why frictional dissipation plays a role in some cases and can be neglected in others remains an open question.

The answer probably relies on the different nature of the polymers used in the experiments. Kendall's experiments were performed with vulcanized ethylene propylene rubber while we used polyvinylsiloxane rubber. Although macroscopic Young's moduli and adhesion energies (corresponding to debonding) are comparable, the dynamics of adhesion may be totally different. Indeed Kendall's procedure required a contact time of 1 h before running a test. The adhesion of PVS to glass seems much faster and our experiments were performed within a few minutes after depositing the polymer on the glass plate. Although the details of the bonding/debonding dynamics are beyond the scope of the present study, our observations suggest that the "bonding" time plays a crucial role in friction.[33] If the adhesion dynamics are slow in comparison with the velocity of the imposed displacement, the elastomer may not re-adhere behind the front, which would lead to the scenario described by Kendall. Conversely, fast re-adhesion would lead to the important friction we observe in our experiments. Capturing all the ingredients involved in the coupling between friction and adhesion will require additional significant efforts. Nevertheless we hope that our study will motivate further studies in the field.

**3.6.2 From catastrophic debonding to friction.** We described in Section 2.3 the theoretical transition from steady peeling to catastrophic debonding in the case of a strip coated with a stiffer backing. This transition is related to the finite stiffness of the backing, which results in shear-lag and the corresponding length scale $\ell_{lag}$ (eqn (4)). The comparison of $\ell_{lag}$ with the length of the adhered strip $L_a$ determines which scenario is expected.

In order to estimate numerical values of the debonding energy $\gamma_s$, we conducted a series of experiments with two different strips covered with a stiffer backing. These strips were covered with a thin mesh of nylon before curing. The imbibition of the mesh assures its firm anchoring to the strip. The effective stiffness $E_b h_b + Eh$ was measured with a standard traction test and it is of the order of $E_b h_b$ instead of $Eh$ for a plain strip of the same thickness. We verified the condition for shear-lag $Eh \ll E_b h_b$. With strips of thickness $h$ = 2 mm, we obtained $\ell_{lag} \simeq$ 20 mm and 30 mm for elastomers of $E$ = 1300 and 225 kPa, respectively.

We followed the lap-shear procedure described by Crosby and collaborators. Force *vs.* displacement tests were carried out on strips adhering over an area $A = L_a w_0$. We measured the critical pulling force $F_C$ and deduced the compliance of the system from the slope of the corresponding curve (see the sketch in Fig. 2a). We represent in Fig. 12 the critical load $F_C$ as a function of $\sqrt{A/C}$. We obtain the expected linear dependence between both quantities for short lengths of adhesion (linear fits in the figure, which provide estimates of the debonding energy $\gamma_s$). However, we observe a clear transition to a different regime for long strips. In this second regime the maximum load increases in a dramatic manner with a value compatible with friction stresses measured independently with plain strips. Interestingly, we find that the transition occurs for $L_a \simeq 2\ell_{lag}$. The description in terms of shear lag is thus also relevant to describe the transition from the regime of catastrophic debonding reported by Crobsy *et al.* to a regime dominated by friction, which is the focus of the present study.

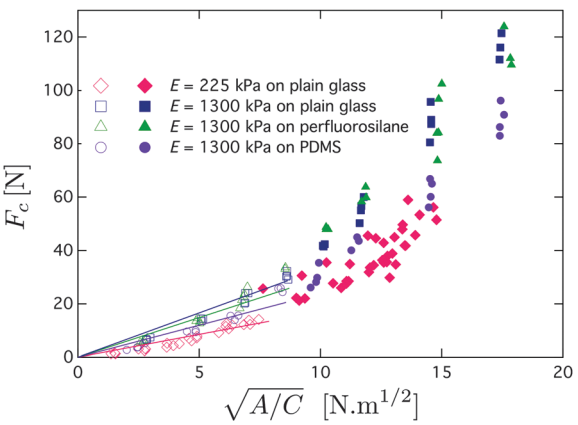


Fig. 12 Experiments with a backing. Critical load $F_C$ as a function of $\sqrt{A/C}$. We observe a transition from catastrophic debonding to the regime dominated by friction as $L_a$ is progressively increased: open symbols $L_a < 2\ell_{lag}$ and filled symbols $L_a > 2\ell_{lag}$. In the first regime, $F_C$ is nearly proportional to $\sqrt{A/C}$. The slope of the corresponding linear fits provides an estimate of the shear debonding energy $\gamma_s$ from eqn (2).

 

# 4 Conclusion

To summarize, the comparison of our experimental results with other studies from the literature put in evidence three different failure modes for a tape adhering to a rigid substrate through molecular interactions.

The first mode involves the coupling between a compliant adhesive and a stiff backing. In this configuration, the whole tape reacts to the load and suddenly detaches if the pulling force exceeds a critical value. This maximum load is proportional to the area of adhesion and a characteristic stress accounting for both adhesion energy and compliance of the system.

The second mode corresponds to tapes consisting of a single compliant strip with slow adhesion dynamics (and consequently low friction). In this case, the peeling force is steady during the peeling process and exhibits a plateau value as the peeling angle vanishes. This force is proportional to the width of the strip and a tension accounting for the adhesion energy and the material stretching modulus. A comparison of the shear lag distance $\ell_{\mathrm{lag}}$ with the length of the strip discriminates between this progressive front propagation and the catastrophic debonding.

Our experiments involve a third scenario where friction plays a crucial role in the peeling process. A sliding front propagates along the adhering part of the strip beyond a threshold, as the other end is progressively pulled away. We developed a simple technique based on monitoring the deformation of the strip to estimate the corresponding friction stress. As a crude approximation, the shear stress is uniform and steady in the zone of friction. The global friction force thus increases linearly with the advance of the sliding front. The strip suddenly detaches when the front eventually reaches its end. The order of magnitude of friction stress estimated for the polyvinylsiloxane elastomers used in our experiments, $\tau \sim 30$ kPa, is in agreement with measurements from the literature regarding studies conducted with other silicone rubbers. In the presence of backing, the criterion based on shear-lag is also relevant to describe the transition from catastrophic debonding to a regime dominated by friction. Although commercial adhesive tapes display more complex behaviors due to the rheology of the adhesive layer[34] or the plasticity of the backing, the current study should be relevant for designing future soft adhesives.

These observations on the role of friction in shear debonding could be interpreted as mode mixity within the traditional frame of fracture mechanics. However, we believe that this terminology might be misleading in our case. Here friction takes place on a very large scale (the whole specimen) and the underlying assumption of a very small process zone where mode mixity takes place is not valid.

Several fundamental questions remain open. The origin of the threshold force remains unclear and should be probed systematically in other configurations. In particular, the implication of friction in the propagation of the front remains to be elucidated. This selection may involve the dynamics of the adhesion process at a molecular scale or, more macroscopically at the scale of roughness of the materials. To investigate the last effect, it would be interesting to carry out experiments on surfaces with patterned geometries such as pillars[27] or wrinkles.[35] Finally our study focuses on the particular lap test configuration. To address most practical applications, it would be interesting to generalize this work to finite peeling angles.

# Acknowledgements

We are grateful to Miguel Trejo, Manoj Chaudhury, Alfred Crosby, Frédéric Restagno, Christophe Poulard, and Chung-Yuen Hui for stimulating discussions on friction of soft polymers. This research was partially funded by the Interuniversity Attraction Poles Programme (IAP 7/38 MicroMAST) initiated by the Belgian Science Policy Office. S. P. thanks the *Becas Chile* program.

# References

1 K. Autumn, M. Sitti, Y. Liang, A. Peattie, W. Hansen, S. Sponberg, T. Kenny, R. Fearing, J. Israelachvili and R. Full, *Proc. Natl. Acad. Sci. U. S. A.*, 2002, **99**, 12252–12256.
2 K. Autumn, A. Dittmore, D. Santos, M. Spenko and M. Cutkosky, *J. Exp. Biol.*, 2006, **209**, 3569–3579.
3 N. Gravish, M. Wilkinson and K. Autumn, *J. R. Soc., Interface*, 2008, **5**, 339–348.
4 T. Endlein, A. Ji, D. Samuel, N. Yao, Z. Wang, W. Barnes, W. Federle, M. Kappl and Z. Dai, *J. R. Soc., Interface*, 2013, **10**, 1–11, DOI: 10.1098/rsif.2012.0838.
5 M. Bartlett, A. Croll, D. King, B. Paret, D. Irschick and A. Crosby, *Adv. Mater.*, 2012, **24**, 1078–1083.
6 M. Bartlett, A. Croll and A. Crosby, *Adv. Funct. Mater.*, 2012, **22**, 4985–4992.
7 J. Risan, A. Croll and F. Azarmi, *J. Polym. Sci., Part B: Polym. Phys.*, 2015, **53**, 48–57.
8 D. Kaelble, *Trans. Soc. Rheol.*, 1959, **III**, 161–180.
9 D. Kaelble, *Trans. Soc. Rheol.*, 1960, **IV**, 45–73.
10 K. Kendall, *J. Phys. D: Appl. Phys.*, 1975, **8**, 1449–1452.
11 K. Kendall, *J. Phys. D: Appl. Phys.*, 1975, **8**, 512–522.
12 B. Newby and M. Chaudhury, *Langmuir*, 1997, **13**, 1805–1809.
13 B. Newby and M. K. Chaudhury, *Langmuir*, 1998, **14**, 4865–4872.
14 N. Amouroux, J. Petit and L. Léger, *Langmuir*, 2001, **17**, 6510–6517.
15 R. Collino, N. Philips, M. Rossol, R. McMeeking and M. Begley, *J. R. Soc., Interface*, 2014, **11**, 20140453.
16 A. Jagota and C. Hui, *Mater. Sci. Eng., R*, 2011, **72**, 253–292.
17 M. Begley, R. Collino, J. Israelachvili and R. McMeeking, *J. Mech. Phys. Solids*, 2013, **61**, 1265–1279.
18 G. Lake and A. Stevenson, *J. Adhes.*, 1981, **12**, 13–22.
19 J. Hutchinson and Z. Suo, *Adv. Appl. Mech.*, 1992, **29**, 64–191.
20 D. King, M. Bartlett, A. Crosby, C. A. Gilman and D. Irschick, *Adv. Mater.*, 2014, **26**, 4345–4351.
21 A. Gent and S. Kaang, *J. Adhes.*, 1987, **24**, 173–181.
22 H. Brown, *Science*, 1994, **263**, 1411–1413.
23 L. Bureau and L. Léger, *Langmuir*, 2004, **20**, 4523–4529.
24 A. Chateauminois and C. Fretigny, *Eur. Phys. J. E: Soft Matter Biol. Phys.*, 2008, **27**, 221–227.

25 A. Chateauminois, C. Fretigny and L. Olanier, *Phys. Rev. E: Stat., Nonlinear, Soft Matter Phys.*, 2010, **81**, 026106.
26 D. Nguyen, PhD thesis, Université Pierre et Marie Curie, 2012.
27 E. Degrandi-Contraires, C. Poulard, F. Restagno and L. Leger, *Faraday Discuss.*, 2012, **156**, 255–265.
28 M. Trejo, C. Fretigny and A. Chateauminois, *Phys. Rev. E: Stat., Nonlinear, Soft Matter Phys.*, 2013, **88**, 052401.
29 S. Mettu and M. Chaudhury, *Langmuir*, 2011, **27**, 10327–10333.
30 M. Barquins, *Mater. Sci. Eng.*, 1985, **73**, 45–63.
31 C. Rand and J. Crosby, *Appl. Phys. Lett.*, 2006, **89**, 261907.
32 S. Ponce, B. Roman, J. Bico and C.-Y. Hui, 2015, in preparation.
33 A. Filippov, J. Klafter and M. Urbakh, *Phys. Rev. Lett.*, 2004, **92**, 135503.
34 R. Villey, C. Creton, P.-P. Cortet, M.-J. Dalbe, T. Jet, B. Saintyves, S. Santucci, L. Vanel, D. Yarusso and M. Ciccotti, *Soft Matter*, 2015, **11**, 3480–3491.
35 C. Rand and A. Crosby, *J. Appl. Phys.*, 2008, **106**, 064913.

 